

WORK OF FRACTURE AND STRAIN-INDUCED COLD CRYSTALLIZATION BEHAVIOR OF AMORPHOUS COPOLYESTER SHEETS

J. Karger-Kocsis^{1*}, *E. J. Moskala*² and *P. P. Shang*²

¹Institute für Verbundwerkstoffe GmbH, Universität Kaiserslautern, P.O. Box 3049, D-67653 Kaiserslautern, Germany

²Eastman Chemical Co., Research Laboratories, P.O. Box 1972, Kingsport, TN 37662-5150, USA

(Received January 20, 2000; in revised form November 20, 2000)

Abstract

The toughness of amorphous copolyester sheets was assessed by the essential work of fracture (EWF) concept. While the yielding-related work of fracture terms did not change significantly, the necking-related parameters strongly decreased with decreasing entanglement density of the copolyesters having different amounts of cyclohexylenedimethylene (*CHDM*) units in their backbones. Furthermore, copolyesters with high *CHDM* content and thus less entanglement density showed full recovery of the necked region beyond the glass transition temperature, i.e. the ‘plastic’ zone in the related specimens formed by cold drawing and not by true plastic deformation. By contrast, the copolyester with negligible amount of *CHDM* did not show this shape recovery. Modulated differential scanning calorimetry (MDSC) revealed that the necking in the latter system was accompanied by strain-induced crystallization. The superior work hardening in the necking stage of the respective poly(ethylene terephthalate) (*PET*) specimens can thus be ascribed to stretching of the entanglement network with superimposed crystallization.

Keywords: amorphous copolyesters, cold crystallization, cold drawing, entanglement, essential work of fracture, modulated DSC, necking

Introduction

The essential work of fracture (EWF) is the most straightforward concept to determine the toughness of ductile polymer sheets and films. The EWF theory ([1–2] and references therein) splits the total energy required to fracture a precracked specimen in two components: the essential (W_e) and the non-essential or plastic work of fracture (W_p), respectively. The first term is needed to fracture the polymer in the process zone and thus to generate new surfaces. W_p is the actual work consumed in the outer plastic region where various energy dissipation mechanisms take place. The total fracture

* Author for correspondence: E-mail: karger@ivw.uni-kl.de

energy, W_f , calculated from the area of the load–elongation curves (Fig. 1), can be expressed by:

$$W_f = W_e + W_p \quad (1)$$

Considering the surface- and volume-dependence of the constituent terms, Eq. (1) can be rewritten into the specific terms:

$$W_f = w_e l t + \beta w_p l^2 t \quad (2)$$

$$w_f = \frac{W_f}{l t} = w_e + \beta w_p l \quad (3)$$

where l is the ligament length, t is the specimen thickness and β is a shape factor related to the form of the plastic zone. Based on Eq. (3), w_e can be estimated from the interception of the linear regression of w_f vs. l plot with the w_f -axis. Hence w_e and βw_p indicate the resistance to crack initiation and propagation, respectively [2]. A deeper insight in the molecular relation of the toughness can be achieved if the specimens used in the test series fully yield along their ligaments prior to the subsequent necking+tearing stage. Such kind of force–elongation behavior (schematically depicted in Fig. 1) allows us to partition between the specific work of fracture required for yielding (w_y) and that consumed by necking (w_n) Fig. 1. As a consequence, the data reduction indicated in Eqs (1–3) are changing for:

$$w_f = w_{f,y} + w_{f,n} = w_e + \beta w_p l \quad (4)$$

$$w_{f,y} = w_{e,y} + \beta' w_{p,y} l \quad (5)$$

$$w_{f,n} = w_{e,n} + \beta'' w_{p,n} l \quad (6)$$

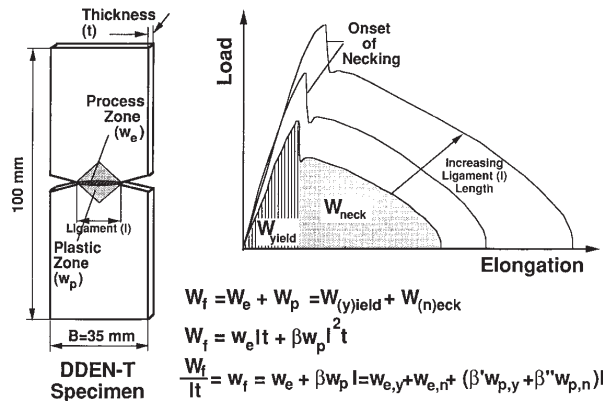


Fig. 1 Scheme of the DDEN-T specimen used along with characteristic load–elongation curves for amorphous copolyesters. Notes: full ligament yielding is marked by a load drop in the load–elongation curves. This figure also outlines the data reduction of the EWF concept

This energy partitioning, introduced by the author's group [3] is well accepted in the meantime. The beauty with this approach is that one can get useful information on how the initial structure and its change due to tensile loading affect the toughness response. By this way the dependence of toughness parameters on molecular and entanglement network characteristics could be clarified in amorphous polymers [4]. In the cited work it has been claimed that the yielding-related work of fracture terms are controlled by the entanglement, whereas the necking-related ones depend additionally on the molecular mass (apart of the loading frequency) affecting the disentanglement process. Nevertheless, it is not yet clear which are the work hardening mechanisms behind the necking. The basic question is whether or not the necking-tearing process depends merely on the network stretchability. The aim of the present paper was to contribute to this issue by assessing the work of fracture parameters for a series of amorphous copolyesters having different tendency to cold (including also the strain-induced) crystallization. The working hypothesis behind this approach is obvious: does crystallization superimpose on the network stretching under given conditions or not? Amorphous copolyesters with various amount of 1,4-cyclohexylenedimethylene (*CHDM*) units in the backbone have been selected as model materials for this study as they show different entanglement densities which affect the cold-crystallization behavior, as well.

Experimental

Materials

Three amorphous copolyester sheets of ca 0.5 mm thickness, provided by Eastman Chemical Co. (Kingsport, TN, USA), were involved in this study. They varied in their *CHDM* content as indicated in Table 1. Table lists also the basic mechanical properties [5]. Note that with increasing *CHDM* content the mean entanglement molecular mass increased and thus the entanglement network density (ν) decreased. The latter was determined by:

$$\nu = \frac{\rho N_A}{M_e} \quad (7)$$

where ρ is the density (Table 1), M_e is the mean entanglement molecular mass and N_A is the Avogadro or Loschmidt number ($6.023 \cdot 10^{23} \text{ mol}^{-1}$).

Table 1 Designation and basic characteristics of the amorphous copolyesters tested

Material, designation	<i>CHDM</i> -content/ mol%	Density/ g cm^{-3}	<i>E</i> -modulus/ GPa	Yield strength/ MPa	Entanglement density, $\nu/10^{25} \text{ m}^{-3}$
<i>PET</i>	<3	1.33	2.4	54.7	25.0...50.8
<i>PETG</i>	≈31	1.27	2.0	48.8	23.5...26.6
<i>PCTG</i>	≈68	1.23	1.8	42.5	~15.7

Notes: the grades of the copolyesters are given in [5], the entanglement density was computed by considering the M_e data from [4]

Based on Table 1 one can recognize that with decreasing ν both the tensile modulus and yield strength decrease, as expected. It should be noted here that with increasing *CHDM* content the tendency to cold crystallization is also hampered.

EFW tests

EFW tests were performed on deeply double edge notched specimens under tensile loading (DDEN-T). The deformation rate was set for 1 mm min^{-1} . Further information to this test along with the data reduction practiced can be taken from our previous papers [2–5]. In order to ascertain whether or not the plastic zone of the DDEN-T specimens (Fig. 1) was caused by cold drawing, the broken specimens were placed few minutes beyond the glass transition temperature (T_g) of the related material in a thermostatic oven. Recall that the complete shape recovery of the plastic zone means that it has been formed by stretching of the entanglement network and not by true plastic (irreversible) deformation. This is the right place to mention that the terminology used in the fracture mechanics is quite misleading as the ‘plastic zone’ (Fig. 1) is not necessarily generated by plastic deformation.

Modulated differential scanning calorimetric (MDSC) study

MDSC traces were taken on samples which were cut from the bulk and plastic zone of the specimens, respectively. The testing conditions were similar as described in our previous paper [6]. However, a heating rate of 5°C min^{-1} modulated by a $\pm 0.531^\circ\text{C } 40 \text{ s}^{-1}$ amplitude was used in this case.

Results and discussion

EFW response and failure behavior

The EFW parameters determined according to Eqs 5 and 6 are listed in Table 2. The present results (also included in [5]) agree very well with previously reported ones achieved earlier on other charges of the same copolyesters [3, 7]. One can notice only a slight change in the yielding-related terms as a function of the *CHDM* content. On the other hand, the necking related terms showed a steep decrease with increasing *CHDM* content or decreasing ν . It means that considerable strain hardening (or more properly work hardening) occurred in those copolyesters the backbone of which was more regular. Hence they have a more pronounced tendency for cold (strain-induced) crystallization. Recall that the non-essential work of fracture parameters, i.e. $w_{e,n}$ and $\beta'' w_{p,n}$, increase with increasing entanglement density. By plotting the non-essential work of fracture parameters as a function of the network density (Table 2) one can notice an overproportional increase for *PET* when the highest literature M_c value was considered in the calculation of the respective ν . This raises the question whether or not the formation of the plastic zone was accompanied by cold recrystallization. Remember that the plastic zone diminished and the original shape of the DDEN-T specimens was fully restored for both *PETG* [3] and *PCTG* [7]. This shape recovery im-

plies that the T_g was not surpassed during deformation and the plastic zone was formed by cold drawing, i.e. merely by stretching of the entanglement network. On the other hand, this shape recovery could not be produced in PET. The shape of the plastic zone did not recover (heal) even when keeping the specimens longer time above T_g (Fig. 2). Note that even under thermal conditions which cause the crystallization of the bulk did not restore the plastic zone (Fig. 2). One can thus suppose that the plastic zone formation was affected by superimposed strain-induced crystallization. This aspect was checked by MDSC.

Table 2 Yielding- and necking-related work of fracture parameters (cf. Eqs (5) and (6)) for the amorphous copolyesters studied

Material code	Work of fracture parameters			
	Yielding		Necking-tearing	
	$w_{e,y}/\text{kJ m}^{-2}$	$\beta'w_{p,y}/\text{MJ m}^{-3}$	$w_{e,n}/\text{kJ m}^{-2}$	$\beta''w_{p,n}/\text{MJ m}^{-3}$
PET	10.3	1.0	35.4	8.9
PETG	13.0	1.4	27.5	6.1
PCTG	10.7	1.8	20.1	3.8

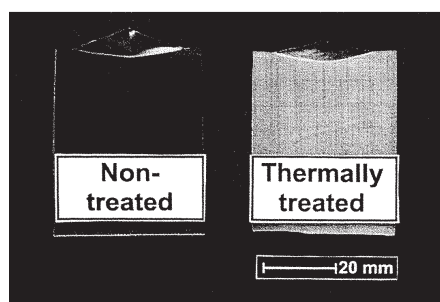


Fig. 2 The same half of a DDEN-T specimen of PET before and after heat treatment ($T=120^\circ\text{C}$, 30 min)

MDSC results

It was demonstrated also by MDSC that the plastic zone in PCTG was formed by cold drawing [6]. The local strain affected the cold crystallization by shifting its onset toward lower temperatures. It was traced to the mechanical loading-induced orientation of the molecules favoring the cold crystallization [6]. The MDSC traces of PETG, that showed the same shape recovery as PCTG, were hardly interpretable [3], thus our efforts were focused on PET. Figure 3 shows characteristic MDSC traces taken from the bulk material. The deconvoluted conventional (C) trace displays the exothermic cold crystallization (peak temperature at $T=137^\circ\text{C}$). The enthalpy of the cold crystallization agrees fairly with that of the subsequent melting which showed a peak at $T=242^\circ\text{C}$ (Fig. 3). This is a strong evidence that the PET was initially amorphous,

indeed. In the reversing (R) trace the T_g at $T=74^\circ\text{C}$ can be well resolved. This T_g step is followed by a broad melting having a peak at $T=240^\circ\text{C}$. The melting enthalpy of the R trace equals with that of the overall crystallization detected by the non-reversing (NR) trace – Fig. 3. Considering this fact along with the observation that the melting starts in the R-curve just after the onset of cold crystallization (C- and NR- traces in Fig. 3), it can be claimed that the *PET* was fully amorphous.

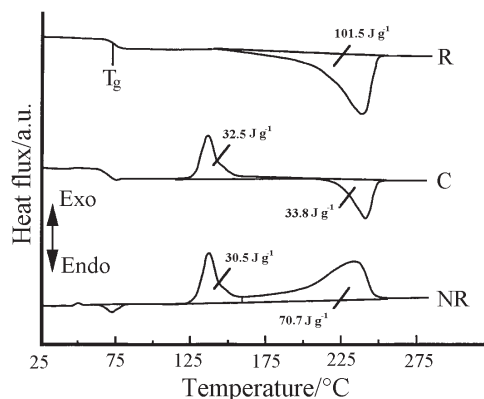


Fig. 3 MDSC curves for the bulk (unstretched) *PET*. Designations: C – conventional, NR – non-reversing and R – reversing components, respectively

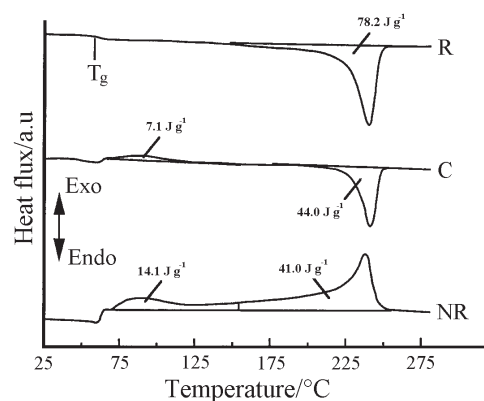


Fig. 4 MDSC curves for the plastic zone (stretched, necked region – Figs 1 and 2) of a DDEN-T specimen of *PET*. For designations cf. Fig. 3

This scenario changes completely in case of samples taken from the deformed plastic zone (Fig. 4). Some cold crystallization can still be resolved in the related C-trace. Note that its peak ($T=91^\circ\text{C}$) lies substantially lower than that of the cold crystallized bulk ($T=137^\circ\text{C}$, Fig. 3). The enthalpy of this cold crystallization process is, however, markedly less than that of the subsequent melting in the C-trace. This suggests that the *PET* in the plastic zone underwent some crystallization during de-

formation. The enthalpy of the melting in the R-curve ($=78.2 \text{ J g}^{-1}$) is markedly larger than the overall crystallization in the NR-traces ($=55.1 \text{ J g}^{-1}$). This is a strong support for the strain-induced crystallization that occurred in the plastic zone of DDEN-T specimens during loading. Comparing the MDSC response of the bulk and plastic zone of *PET* (Figs 3 and 4), one can notice that the cold crystallization was shifted toward lower temperatures due to the molecular orientation involved. This orientation triggered the crystallization of *PET*. The overlapping of the cold crystallization with the T_g is likely responsible for the apparent shift in the T_g and for its peculiar appearance (R- and NR-traces in Fig. 4). The authors are not aware of the reasons of the changes in the T_g step. Note that a significant decrease in the cold crystallization temperature was found due to the orientation (uni- or biaxial type) of *PET* as demonstrated several times earlier [8]. A high orientation in the amorphous phase facilitates the crystallization of *PET* at lower temperatures, however, usually above the T_g . Recall that our results indicate substantial crystallization below the T_g of the bulk *PET*. Hence, strain-induced crystallization can be made responsible for the overproportional high necking related terms ($w_{c,n}$ and $\beta''w_{p,n}$, Table 2) in *PET*. As the plastic zone of *PET* remained transparent after crystallization (and not became opaque as expected) the size of the crystallites should lay below that of the wavelength of the visible light. The presence of microcrystallinity could be evidenced by X-ray scattering. There is still one discrepancy to be solved: crystallization is accompanied with heat release and thus work softening instead of the observed hardening. First, the strain-induced crystallization in the plastic zone is limited. By assuming 140 J g^{-1} melting enthalpy for the fully crystalline *PET* [9] and by deducing the cold crystallization from the enthalpy of subsequent melting in the C-trace of Fig. 4, ca. 26% crystallinity can be estimated. When one deduces the overall NR-crystallization from the overall R-melting, the mean crystallinity becomes even less, viz. 17%. Second, the crystallization is limited also in size (microcrystallization took place as argued above). Third, the crystalline domains formed are converting the *PET* into a special thermoplastic elastomer the structure of which consists of an entanglement network having some extra nodes in form of crystalline domains. The authors think that this structural model would be helpful to understand the stress oscillation phenomena often reported for *PET* [10]. Note that the opaque/transparent striation pattern perpendicular to the loading direction was ascribed to a stick-slip mechanism caused by periodical work hardening (network stretching+crystallization – stick stage) and work softening by release of the crystallization heat (slip stage) [11]. No such stress oscillation could be achieved, however, for *PETG* and *PCTG* both of which show less tendency for strain-induced crystallization than *PET*. The structural model proposed above can also explain why the overall crystallinity of the stretched plastic zone is less than that of the unstretched bulk (compare the R melting enthalpy values in Figs 3 and 4). The supposed physical network having ‘knots’ from entanglements and crystallized microdomains retards the chain movement and its ordering in the crystalline lattice during heating.

Conclusions

Based on this study devoted to clarify the relation between necking-related work of fracture terms and network characteristics in amorphous copolyesters showing different tendency for cold (strain-induced) crystallization the following conclusions can be drawn:

– the resistance to necking, characterized by the necking-related work of fracture parameters, resulted in the ranking: *PET*>*PETG*>*PCTG*. This ranking is in line with a similar change in respect to the entanglement densities.

– the plastic zone in *PETG* and *PCTG* specimens formed by network stretching. It was evidenced by full recovery of the plastic zone when the specimens were kept beyond the T_g of the material for a short period of time.

– no plastic zone recovery could be produced in *PET*. This was attributed to strain-induced crystallization superimposed on the network stretching based on MDSC results. The related network having ‘knots’ of entanglements and microcrystallized domains was traced for the outstanding necking resistance of *PET*.

* * *

This work contains results achieved by grants supported by the German Science Foundation (DFG). The authors thank to Dr. D. E. Mouzakis for performing the EWF tests. JKK would like also to thank the Fonds der Chemischen Industrie for the support of his personal research.

References

- 1 Y. W. Mai, S.-C. Wong and X.-H. Chen, Application of fracture mechanics for characterization of toughness of polymer blends in ‘Polymer Blends: Vol. 2. Performance’, (Eds: D. R. Paul and C. B. Bucknall), Wiley, New York 2000, p. 17.
- 2 J. Karger-Kocsis, Microstructural and molecular dependence of the work of fracture parameters in semicrystalline and amorphous polymer systems in ‘Fracture of Polymers, Composites and Adhesives’ (Eds.: J. G. Williams and A. Pavan), Elsevier, Oxford 2000, p. 213.
- 3 J. Karger-Kocsis and E. J. Moskala, *Polym. Bull*, 39 (1997) 503.
- 4 J. Karger-Kocsis, Fracture and fatigue behavior of amorphous (co)polyesters as a function of molecular and network variables in ‘Handbook of Thermoplastics Polyesters’, (Ed.: S. Fakirov), Wiley-VCH, Weinheim 2001, in press.
- 5 D. E. Mouzakis, J. Karger-Kocsis and E. J. Moskala, *J. Mater. Sci. Letters*, 19 (2000) 1615.
- 6 J. Karger-Kocsis, P. P. Shang and E. J. Moskala, *J. Therm. Anal. Cal.*, 55 (1999) 21.
- 7 J. Karger-Kocsis, T. Czigány and E. J. Moskala, *Polymer*, A9 (1998) 3939.
- 8 K. Nakayama and K. Qi, *Polym. Polym. Compos.*, 8 (2000) 387.
- 9 A. Mehta, U. Gaur and B. Wunderlich, *J. Polym. Sci. Part B.: Phys.*, 16 (1978) 289.
- 10 H. Ebener, B. Pleuger and J. Petermann, *J. Appl. Polym. Sci.*, 71 (1999) 813.
- 11 J. Karger-Kocsis, O. I. Benevolenski and E. J. Moskala, *J. Mater. Sci.*, 37 (2001), in press.